Hindawi Publishing Corporation
EURASIP Journal on Wireless Communications and Networking
Volume 2009, Article ID 909075, 14 pages
doi:10.1155/2009/909075

Research Article

Multiple CFOs in OFDM-SDMA Uplink: Interference Analysis and Compensation

Malte Schellmann and Volker Jungnickel

Fraunhofer Institute for Telecommunications, Heinrich-Hertz-Institut, Einsteinufer 37, 10587 Berlin, Germany

Correspondence should be addressed to Malte Schellmann, schellmann@hhi.fraunhofer.de

Received 1 July 2008; Revised 14 November 2008; Accepted 11 March 2009

Recommended by Erdal Panayirci

In OFDM-based space division multiple access (SDMA) systems, multiple users are served by a multiantenna base station simultaneously on the same frequency resources. In the uplink, each user's signal may be distorted by an independent carrier frequency offset (CFO), which impairs the orthogonality of the subcarrier signals and, if not properly compensated, results in performance degradations. We analyze the influence of multiusers' CFOs on the signal transmission in the OFDM-SDMA uplink and derive suitable bounds for the achievable signal-to-interference conditions. By modifying the signal model suitably, we develop a simple scheme for partial compensation of the CFO distortions. It allows to maintain the subcarrier-wise channel equalization and thus is well suited to be applied for a real-time system implementation. However, as CFOs impair the cyclic structure of the OFDM symbols, our scheme is not able to compensate for the entire distortion. The remaining interference is treated as additional noise, which limits the supported size of the CFOs.

1. Introduction

A promising solution to lead wireless communication systems toward high spectral efficiencies is the combination of the orthogonal frequency division multiplexing (OFDM) together with the space-division multiple access (SDMA) technique [1]. In the SDMA uplink, multiple users communicate simultaneously with a multiantenna base station (BS) on the same frequency resources by transmitting their signals on different spatial layers. OFDM is a favored technique for the transmission in frequency-selective channels, as it facilitates the equalization process while at the same time enabling high spectral efficiencies. However, one of its deficiencies is its high sensitivity towards time-variant distortions. In general, these destroy the orthogonality of the single subcarrier signals and give rise to the so-called intercarrier interference (ICI), limiting the achievable system performance [2, 3]. One source for time-variant distortions is the carrier frequency offset (CFO), owing to a mismatch between the oscillators at the transmitter and receiver sides. While estimation and compensation of CFO distortions in a single user link are fairly easy and conveniently solved [4–6], coping with different CFOs from multiple users in any OFDM-based multiuser uplink is much more challenging, as all CFOs need to be estimated independently, and the conventional techniques for compensation do not apply.

The influence of CFOs from multiple users in an OFDM-based uplink has been studied extensively in the context of OFDMA systems, where simultaneous access is granted to multiple users by individually assigning distinct sets of subcarriers to them [7–9]. An overview of existing synchronization techniques together with a sound summary of the general requirements for uplink synchronization can be found in [10]. Estimation of multiple users' CFOs can be performed based on blind techniques exploiting specific properties of the utilized OFDM signals and their statistics [11–15] or based on pilot-based techniques [16, 17]. For CFO compensation, the simplest approach is to feed back the estimated CFO to the corresponding user terminal, so that it may adapt its oscillator accordingly or apply a precompensation to its transmit signal [11]. However, the drawback of this feedback approach is that large delays may

occur before the CFOs are properly compensated. There also exist some proposals for CFO compensation to be carried out directly at the receiver by adequate signal processing. These approaches are either based on the inversion of a high dimensional matrix representing the ICI-affected channel for a complete OFDMA symbol [18, 19], or they make use of successive interference cancelation techniques [20], which may be performed in an iterative fashion [21]. Unfortunately, all these approaches result in a significant increase of computational complexity compared to common OFDM processing, whose favorable property is to enable an independent subcarrier-wise processing. Although the complexity of the aforementioned approaches based on matrix inversion can be further reduced if specific properties of the signal model are exploited [15, 22, 23], it still remains considerable. A suboptimum solution maintaining the subcarrier-wise signal processing at the receiver is presented in [24]. The user signals are separated first, whereafter they are individually compensated for their user-specific CFO. Although not all ICI can be removed, a satisfactory performance is achieved if the CFOs do not become too large.

The major difference in OFDM-SDMA systems is that the channel is enhanced by a spatial dimension. To separate the users' signals, knowledge of the SDMA channel per subcarrier is required. With CFO distortions present, solutions to estimate the SDMA channel have been proposed in [25, 26]; joint estimation of SDMA channels and the users' CFOs can be found in [27–29]. Contributions [26, 28] also provide approaches to compensate for the CFO distortions at the receiver, which, however, have complexity demands that are similar to the OFDMA techniques mentioned earlier.

The work in this paper was motivated by seeking for a simple receiver-based CFO compensation method for the uplink of an OFDM-SDMA system. Hereby, the subcarrier-wise channel equalization is supposed to be maintained to facilitate implementation in a real-time system. Therefore, we resort to the basic idea from [24] and develop a system concept where the user signals are first separated by common OFDM-SDMA equalization and compensated for their individual CFO distortions afterwards. As this approach is clearly suboptimum, the major focus of our work lies in the proper analysis of the achievable signal conditions with respect to the amount of interference that remains in the system after such compensation. In particular, we derive closed-form expressions characterizing the bounds for the signal-to-interference ratio (SIR) before and after CFO compensation, which are verified by numerical bit-error rate analysis. This way, we obtain insights into the suitability of the approach and reveal the limits of its application range.

Based on our results, it turns out that the proposed CFO compensation concept operates conveniently only if the size of the CFOs present in the system can be kept below a few percent of the subcarrier spacing. Therefore, the approach has to be seen as a technique for fine-synchronization. Correspondingly, a coarse-frequency synchronization of all users' signals has to be ensured. This coarse synchronization can be achieved by a frequency-advance, where terminals precompensate their signals with the CFO estimated in the downlink phase. The concept of frequency-advance was recently realized in a practical system, as reported in [30]. In [31], we already presented the basic idea of this work and initial analytical results. Here we extend the analysis to support linear receivers providing spatial diversity gains, add the case of noncompensated CFOs for illustrative comparison and provide a refined update of the CFO compensation process to be carried out in frequency domain, which facilitates implementation.

The paper is structured as follows: Section 2 introduces the OFDM signal model based on vector notation. As a preparation for analysis of the OFDM-SDMA system, we determine the SIR conditions for a single antenna OFDM link in Section 3. Hereafter, the model is modified to form the basis for the simplified CFO compensation process in OFDM-SDMA systems. In Section 4, we analyze the SIR conditions in the OFDM-SDMA system and derive bounds for the two cases where CFOs are compensated according to the proposed scheme and where they are not. These bounds are verified by simulation results in Section 5.

2. Signal Model

Notation. We use bold capital letters to denote matrices and bold letters for vectors. Scalars are written in italics. $(\cdot)^H$ and $(\cdot)^*$ denote conjugate transpose and conjugate operator, respectively. $\mathrm{tr}(\cdot)$ refers to the trace operator. $\mathrm{diag}(\mathbf{x})$ represents a diagonal matrix, whose diagonal is constituted of vector $\mathbf{x}$. $E\{\cdot\}$ denotes the expectation operator.

2.1. Vector Notation of OFDM. Consider an OFDM system with a total of N subcarriers. The transmission equation for a CFO-distorted single-input single-output (SISO) link is given by

$$\mathbf{y} = \mathbf{F}\mathbf{P}_2\mathbf{C}(\varphi)\mathbf{H}\mathbf{P}_1\mathbf{F}^H \cdot \mathbf{x}, \tag{1}$$

$\mathbf{x}$ is the data vector comprising the N data symbols constituting the OFDM symbol, $\mathbf{F}$ is the $N \times N$ discrete Fourier transform (DFT) matrix, and $\mathbf{P}_1$ and $\mathbf{P}_2$ are permutation matrices used to append and cut the cyclic prefix (CP) of length N_g samples. Further, $\mathbf{H}$ is the $(N + N_g) \times (N + N_g)$ Toeplitz channel matrix constituted from the channel impulse response (CIR) h_l, $l \in \{0, \ldots, L\}$, where $L \leq N_g$. Finally,

$$\mathbf{C}(\varphi) = \mathrm{diag}\left(\left[\exp\left(-j\varphi N_g\right) \;\cdots\; \exp\left(j\varphi(N-1)\right)\right]\right) \tag{2}$$

is the CFO distortion matrix, where the phase rotation factor φ is defined as $\varphi = 2\pi\omega/N$, with $\omega \in [-0.5, 0.5]$ being the CFO normalized to the subcarrier spacing. For $\varphi = 0$ (no CFO), the effective channel

$$\mathbf{F}\mathbf{P}_2\mathbf{H}\mathbf{P}_1\mathbf{F}^H = \mathbf{\Lambda} \tag{3}$$

yields a diagonal matrix, whose elements on the diagonal λ_k, $k \in \{1, \ldots, N\}$, represent the N-point DFT of the CIR h_l. By a few simple transformations, the diagonal matrix $\mathbf{\Lambda}$ can be restored in (1), yielding

$$\mathbf{y} = \mathbf{F}\overline{\mathbf{C}}(\varphi)\mathbf{F}^H\mathbf{F}\mathbf{P}_2\mathbf{H}\mathbf{P}_1\mathbf{F}^H \cdot \mathbf{x} = \mathbf{U}\mathbf{\Lambda} \cdot \mathbf{x}, \tag{4}$$

where we introduced

$$\overline{\mathbf{C}}(\varphi) = \operatorname{diag}([1 \ \exp(j\varphi) \cdots \exp(j\varphi(N-1))]),$$
$$\mathbf{U} = \mathbf{F}\overline{\mathbf{C}}(\varphi)\mathbf{F}^H. \tag{5}$$

Note that $\mathbf{F}$ is unitary thus $\mathbf{F}^H\mathbf{F}$ equals the identity matrix $\mathbf{I}$.

2.2. OFDM-SDMA Signal Model. Next the focus is turned to an OFDM-SDMA system, where Q single-antenna terminals transmit their signals simultaneously to an M-antenna base station on the same frequency resource. The users' transmission signals propagate via different paths and will be marked with different spatial signatures, which enable the multiantenna receiver to separate and recover the users' transmission signals.

For the system model, the OFDM signal vectors $\mathbf{x}_q$, $q \in \{1,\ldots,Q\}$ from the Q users are stacked into one large vector $\bar{\mathbf{x}}$ of dimension QN. Correspondingly, the M OFDM reception vectors $\mathbf{y}_m$ are stacked into one large vector $\bar{\mathbf{y}}$. Each user may have an individual CFO, resulting in Q different CFO distortion matrices $\mathbf{U}_q$, which are generated from individual phase factors $\varphi_q = 2\pi\omega_q/N$. For simplicity, let us assume the number of users to be $Q = 2$. Based on the signal model in (4), the transmission equation in the OFDM-SDMA system reads

$$\underbrace{\begin{pmatrix}\mathbf{y}_1\\ \vdots \\ \mathbf{y}_M\end{pmatrix}}_{\bar{\mathbf{y}}} = \underbrace{\begin{pmatrix}\mathbf{U}_1\boldsymbol{\Lambda}_{11} & \mathbf{U}_2\boldsymbol{\Lambda}_{12}\\ \vdots & \vdots \\ \mathbf{U}_1\boldsymbol{\Lambda}_{M1} & \mathbf{U}_2\boldsymbol{\Lambda}_{M2}\end{pmatrix}}_{\mathbf{H}_C} \cdot \underbrace{\begin{pmatrix}\mathbf{x}_1\\ \mathbf{x}_2\end{pmatrix}}_{\bar{\mathbf{x}}}, \tag{6}$$

where each of the single user/receive antenna links is characterized by its own diagonal channel matrix $\boldsymbol{\Lambda}_{mq}$.

2.3. Statistical Channel Model. Within this paper, we will assume Rayleigh-fading conditions for the discrete CIR, meaning that the channel coefficients h_l are drawn independently from complex Gaussian distributions with mean power σ_l^2. For $l \in \{0,\ldots,L\}$, $\sigma_l^2 = E\{|h_l|^2\}$ represents the power delay profile (PDP) of the channel, which is assumed to be monotonically decreasing for increasing l. Furthermore, we assume the channel to be passive, that is, the sum of the mean powers of all channel coefficients is equal to unity, $\sum_{l=0}^{L}\sigma_l^2 = 1$. To specify suitable bounds within our analysis, we will frequently use a uniform PDP with constant power for all channel taps, which is defined as $\sigma_l^2 = 1/(L+1)$ for all l. From these assumptions, it follows for the subcarrier channels λ_k that they behave like random variables which are drawn from complex Gaussian distributions with unit power. The correlation between the channels at adjacent subcarrier positions is characterized by the frequency-domain autocorrelation function $r(\kappa)$, $\kappa \in \{0,\ldots,N-1\}$, where κ refers to the distance between subcarriers. $r(\kappa)$ is obtained from the N-point DFT of the PDP, that is,

$$r(\kappa) = \sum_{l=0}^{L}\sigma_l^2 \ \exp\left(-\frac{j2\pi l\kappa}{N}\right), \quad \kappa \in \{0,\ldots,N-1\}. \tag{7}$$

In the OFDM-SDMA system, the channels of the QM single antenna links are characterized by the same statistical properties, but are assumed to be statistically uncorrelated. In particular, we assume all channels to have identical channel length L and identical PDP, which may be reasonable for user terminals experiencing non-line-of-sight (NLOS) multipath fading.

3. Analysis of Single-Antenna OFDM Link

To prepare analysis of the SIR conditions in the OFDM-SDMA system, we focus in this section on a separate single-antenna OFDM link. In the following, we analyze the impact of CFO distortions and derive a bound for the SIR (Section 3.1). To enable a simplified equalization process in the OFDM-SDMA system, where the user signals are first spatially separated and thereafter individually compensated for their CFO distortions, we modify this signal model accordingly (Section 3.2). This model introduces an additional error term, which cannot be compensated by simple means. Hence, its power and the resulting SIR conditions are analyzed in Section 3.3. The proper process for partial compensation of the CFO distortions after channel equalization is then presented in Section 3.4.

3.1. Impact of CFO Distortions. In (4), matrix $\mathbf{U} = \mathbf{F}\overline{\mathbf{C}}(\boldsymbol{\varphi})\mathbf{F}^H$ is a circular matrix, whose rows are circularly shifted versions of $u(\kappa)$ being the DFT of the diagonal in $\overline{\mathbf{C}}(\varphi)$, that is,

$$u(\kappa) = \frac{1}{N}\sum_{n=0}^{N-1}\exp\left(j2\pi\omega\frac{n}{N}\right)\exp\left(j2\pi\frac{\kappa n}{N}\right) \tag{8}$$

with $\kappa \in \{0,\ldots,N-1\}$. The aforementioned expression represents a geometric series, and hence it can be simplified to [32]

$$u(\kappa) = \frac{1}{N}\exp\left(j\pi(\omega+\kappa)\frac{N-1}{N}\right)\frac{\sin(\pi(\omega+\kappa))}{\sin(\pi(\omega+\kappa)/N)}. \tag{9}$$

As the DFT is periodic, the definition range may be changed to $\kappa \in \{-N/2,\ldots,N/2-1\}$. By doing so, we can use an approximation for large N based on the si-function $\operatorname{si}(x) = \sin(x)/x$, so that $u(\kappa)$ can be given as

$$u(\kappa) = (-1)^{\kappa}\exp(j\pi\omega)\cdot \operatorname{si}(\pi(\omega+\kappa)). \tag{10}$$

Multiplying the circular matrix $\mathbf{U}$ with a frequency-domain signal vector represents a cyclic convolution of that signal vector with function $u(\kappa)$, which introduces the ICI. For $\kappa \neq 0$, $u(\kappa)$ specifies the amount of ICI, that is, induced on any subcarrier from a subcarrier signal which is spaced κ subcarriers apart. $u(0)$ itself represents the attenuation of the power of each subcarrier signal. From (10), we observe that multiplication with function $u(\kappa)$ imposes a constant phase rotation $\exp(j\pi\omega)$ on all subcarrier signals. This constant phase factor corresponds to the mean CFO-induced phase rotation observed over the total duration of the time-domain OFDM symbol of N samples length. It is also referred to as the common phase error (CPE) induced by the CFO distortions.

Next, we will examine the mean power of the ICI and the resulting SIR. From (4), the received signal y_k at subcarrier position $k \in \{1, \ldots, N\}$ can with the aforementioned results be written as

$$y_k = u(0)\lambda_k x_k + \sum_{j=1, j\neq k}^{N} u(j-k)\lambda_j x_j, \tag{11}$$

where x_k denotes the transmit symbol at subcarrier k. The first term in the aforementioned equation denotes the useful signal received at subcarrier k, while the second term represents the ICI from all other subcarriers. Let the transmit symbols x_k be independent and identically distributed (i.i.d.) with constant mean power P_s. Then, as $E\{|\lambda_k|^2\} = 1$, the mean power of the useful signal P_u at subcarrier k amounts to $P_u = P_s|u(0)|^2$. Furthermore, the mean power of the ICI from all other subcarriers distorting the useful signal yields $P_{\mathrm{ICI}} = P_s \sum_{j=1}^{N-1} |u(j)|^2$, which can be upper bounded by $P_s(1 - |u(0)|^2)$. This bound is tight in case all N available subcarriers are occupied with data symbols. Using (10), we can lower bound the SIR resulting from the ICI as follows [3]:

$$\mathrm{SIR}_{\mathrm{ICI}} = \frac{P_u}{P_{\mathrm{ICI}}} \geq \frac{\mathrm{si}^2(\pi\omega)}{1 - \mathrm{si}^2(\pi\omega)}. \tag{12}$$

3.2. Modified Model for Simplified Equalization in SDMA. The common method to compensate distortions from a single CFO is to rotate the phase φ in the received time-domain signal back to zero prior to any DFT operation [33]. Afterwards, the diagonal channel $\mathbf{\Lambda}$ can be equalized subcarrier-wise, as common in OFDM. As already mentioned, this proceeding is not applicable in OFDM-SDMA systems, as compensating for the CFO of a single user would misalign the signal of any other user. However, to maintain the simplified subcarrier-wise equalization OFDM systems are favored for, it would be desirable to interchange the order of compensation and equalization operation, so that the user signals can first be separated and compensated for their individual CFOs afterwards. This approach requires a modification of the signal model (1), where the CFO distortion matrix $\mathbf{U}$ should be moved to the right hand side of channel matrix $\mathbf{H}$. To achieve that, we insert the matrix product $\mathbf{C}(-\varphi)\mathbf{C}(\varphi) = \mathbf{I}$ into (1) to the right next to $\mathbf{H}$ and obtain

$$\mathbf{y} = \mathbf{F}\mathbf{P}_2\overline{\mathbf{H}}\mathbf{C}(\varphi)\mathbf{P}_1\mathbf{F}^H \cdot \mathbf{x} \tag{13}$$

with the modified channel matrix $\overline{\mathbf{H}} = \mathbf{C}(\varphi)\mathbf{H}\mathbf{C}(-\varphi)$. This matrix has the same structure as the original $\mathbf{H}$, but the channel coefficients are now modified according to $\overline{h}_l = h_l \cdot \exp(j\varphi l)$. The corresponding diagonal matrix $\overline{\mathbf{\Lambda}}$ in frequency domain results from (3) based on $\overline{\mathbf{H}}$, that is,

$$\overline{\mathbf{\Lambda}} = \mathbf{F}\mathbf{P}_2\overline{\mathbf{H}}\mathbf{P}_1\mathbf{F}^H. \tag{14}$$

Correspondingly, the diagonal of $\overline{\mathbf{\Lambda}}$ represents the DFT of $\overline{h}_l$.

To restore the diagonal matrix $\overline{\mathbf{\Lambda}}$ in (13), the term $\mathbf{P}_1\overline{\mathbf{C}}(\varphi)$ has to be used instead of $\mathbf{C}(\varphi)\mathbf{P}_1$, with $\overline{\mathbf{C}}(\varphi)$ as defined in (5). The difference between these two terms amounts to

$$\mathbf{\Gamma} = \mathbf{C}(\varphi)\mathbf{P}_1 - \mathbf{P}_1\overline{\mathbf{C}}(\varphi). \tag{15}$$

Matrix $\mathbf{\Gamma}$ will in the following be denoted as the error matrix, as it represents the error that will be introduced if the two matrix products are replaced directly. Its structure will be characterized succeedingly. Recall that the $(N + N_g) \times N$ dimensional matrix $\mathbf{P}_1$ appends a cyclic prefix of N_g samples to the N-dimensional input vector $\mathbf{x}$; hence its structure can be described by an $N_g \times N_g$ identity matrix which is located in the upper right corner on top of an $N \times N$ identity matrix, and all other elements being zero. The structure of the error matrix $\mathbf{\Gamma}$ thus contains mainly zeros except in its upper right $N_g \times N_g$ submatrix, which itself is a diagonal matrix whose diagonal is composed of the elements γ_n, $n \in \{-N_g, \ldots, -1\}$, with

$$\gamma_n = \exp(jn\varphi)\left(1 - \exp(jN\varphi)\right). \tag{16}$$

Plugging $\mathbf{C}(\varphi)\mathbf{P}_1 = \mathbf{P}_1\overline{\mathbf{C}}(\varphi) + \mathbf{\Gamma}$ into (13) now yields

$$\mathbf{y} = \overline{\mathbf{\Lambda}} \cdot \underbrace{\mathbf{F}\overline{\mathbf{C}}(\varphi)\mathbf{F}^H}_{\mathbf{U}} \cdot \mathbf{x} + \underbrace{\mathbf{F}\mathbf{P}_2\overline{\mathbf{H}}\mathbf{\Gamma}\mathbf{F}^H}_{\mathbf{V}} \cdot \mathbf{x}. \tag{17}$$

The first part of the equation exhibits the desired signal structure, where the location of the CFO distortion and channel transmission operations have been interchanged compared to (4). Thus, the suggested receiver processing can be enabled. However, we have an additive error term $\mathbf{V}\mathbf{x}$ generated from the error matrix $\mathbf{\Gamma}$. The inner product $\mathbf{P}_2\overline{\mathbf{H}}\mathbf{\Gamma}$ of this term is a matrix with mainly zero elements except in its upper right $L \times L$ submatrix $\mathbf{V}_u$. This submatrix is an upper triangular matrix with the following structure:

$$\mathbf{V}_u = \begin{pmatrix} \gamma_{-L} \cdot \overline{h}_L & \gamma_{-L+1} \cdot \overline{h}_{L-1} & \cdots & \gamma_{-1} \cdot \overline{h}_1 \\ 0 & \gamma_{-L+1} \cdot \overline{h}_L & & \gamma_{-1} \cdot \overline{h}_2 \\ \vdots & & \ddots & \vdots \\ 0 & 0 & & \gamma_{-1} \cdot \overline{h}_L \end{pmatrix}. \tag{18}$$

We observe that the elements in this submatrix reflect the (complex) difference of the effective channel echoes seen by the samples in the CP and their cyclic repetition at the end of the OFDM symbol. If these two signal fractions are no longer identical owing to the CFO, the periodic property of the OFDM signals is violated, resulting in interference to all subcarrier signals. With this finding, the total CFO-induced interference contained in model (17) can be segregated into two different types: the first type is given as ICI of the original subcarrier signal in $\mathbf{x}$, generated by the cyclic convolution in $\mathbf{U}$, and the second type is given as interference caused by the violation of the periodicity of the OFDM signals, represented in the term $\mathbf{V}\mathbf{x}$.

If equalization and CFO compensation are carried out as described earlier, the power from $\mathbf{V}\mathbf{x}$ will remain in the system and distort the signal as interference. In the following, we will therefore analyze its power as well as the resulting SIR conditions.

3.3. Interference Remaining after CFO Compensation. Obviously, $\mathbf{V}$ is the all-zero matrix if $\varphi = 0$ (i.e., no CFO is present) or if the channel is frequency flat ($L = 0$).

Otherwise, the total power contained in $\mathbf{Vx}$ depends on the actual number of the channel echoes L. The mean power P_V contained in this term can be calculated by

$$P_V = \operatorname{tr}\left(E\left\{\mathbf{V}\mathbf{x}\mathbf{x}^H\mathbf{V}^H\right\}\right). \tag{19}$$

The expression given in the argument of the trace operator represents the correlation matrix $\mathbf{R}_e$ of the error term $\mathbf{Vx}$. As the elements constituting $\mathbf{V}$ and $\mathbf{x}$, respectively, can be considered to stem from independent stochastic processes, we may write

$$\mathbf{R}_e = E\left\{\mathbf{V}\mathbf{x}\mathbf{x}^H\mathbf{V}^H\right\} = E\left\{\mathbf{V}E\left\{\mathbf{x}\mathbf{x}^H\right\}\mathbf{V}^H\right\}. \tag{20}$$

With the i.i.d. assumption for the symbols contained in $\mathbf{x}$ with mean power P_s, $E\{\mathbf{x}\mathbf{x}^H\}$ is a diagonal matrix scaled with P_s. In case all subcarriers are occupied with data symbols, it equals $P_s \cdot \mathbf{I}$, and we obtain $\mathbf{R}_e = P_s \cdot E\{\mathbf{V}\mathbf{V}^H\}$. Inserting the matrix product constituting $\mathbf{V}$ from (17) and considering the structure of the inner product $\mathbf{P}_2\overline{\mathbf{H}}\mathbf{\Gamma}$ with its submatrix $\mathbf{V}_u$, the power P_V yields

$$P_V = \operatorname{tr}(\mathbf{R}_e) = P_s \cdot E\left\{\operatorname{tr}\left(\mathbf{V}_u\mathbf{V}_u^H\right)\right\}. \tag{21}$$

With $\mathbf{V}_u$ from above, we obtain

$$\operatorname{tr}\left(\mathbf{V}_u\mathbf{V}_u^H\right) = 4\sin^2(\pi\omega)\sum_{m=1}^{L}\sum_{l=m}^{L}|h_l|^2, \tag{22}$$

where the expression $4\sin^2(\pi\omega)$ results from $|\gamma_n|^2$. Taking the expected value of this expression relates P_V to fractions of the channel's PDP. Resorting to the characteristics of the considered channel model given in Section 2.3, we can upper bound P_V according to

$$P_V \le P_s L \cdot 2\sin^2(\pi\omega), \tag{23}$$

where the relation holds with equality for a uniform PDP.

Once we know the total power of the interference generated by the error matrix $\mathbf{\Gamma}$, we examine next how this interference power affects the single subcarrier signals. For this purpose, we first focus on the correlation of this additive interference in the frequency domain. The structure of matrix $\mathbf{V}_u$ reveals that the interference affects only the first L samples of the time-domain OFDM symbol, hence the interference in frequency domain will be highly correlated. To obtain more insight, we focus on the $N \times N$-dimensional time-domain correlation matrix, which we obtain from (20) as $\mathbf{R}_{e,t} = \mathbf{F}^H\mathbf{R}_e\mathbf{F} = E\{\mathbf{P}_2\overline{\mathbf{H}}\mathbf{\Gamma}\mathbf{\Gamma}^H\overline{\mathbf{H}}^H\mathbf{P}_2^H\}P_s$. As the channel taps $\overline{h}_l$ in $\overline{\mathbf{H}}$ are uncorrelated, $\mathbf{R}_{e,t}$ is a diagonal matrix with its diagonal representing the time-domain interference power profile $r_{e,t}(n)$. Only the first L elements of $r_{e,t}(n)$ differ from zero and are proportional to partial sums of the PDP:

$$r_{e,t}(n) \sim \sum_{l=n}^{L}\sigma_l^2 \le 1 - \frac{n}{L+1}, \quad n \in \{1,\ldots,L\}. \tag{24}$$

The values of $r_{e,t}(n)$ can be bounded according to the expression on the right-hand side, holding with equality for a uniform PDP. The frequency correlation matrix $\mathbf{R}_e = \mathbf{F}\mathbf{R}_{e,t}\mathbf{F}^H$ now is circular, which means the correlation between the subcarriers is independent of the actual subcarrier position k. We thus conclude that the mean interference power P_i that distorts each subcarrier signal amounts to

$$P_i(\omega) = P_V/N \le P_s L \cdot 2\sin^2(\pi\omega)/N, \tag{25}$$

indicating that the mean interference power P_V is uniformly spread over all the subcarrier signals.

To find out the correlation of the interference over frequency, we can determine the frequency correlation function $r_e(\kappa)$, which is calculated from the N-point DFT of the time-domain interference power profile $r_{e,t}(n)$. According to (24), $r_{e,t}(n)$ can be represented by a linear function with slope $\beta = (L+1)^{-1} \le 0.5$ which is multiplied by a rectangular window of width L to confine it to the specified range. The corresponding frequency correlation function $r_e(\kappa)$ thus can be generated by a convolution of the DFT of that linear function with the DFT of the rectangular window. It is quite evident that for the constrained slope β, the rectangular function will dominantly influence the spread of the correlation function, and hence we restrict our inspection on this component only. The DFT of the rectangular function of width L is

$$r_e(\kappa) \sim \frac{1}{N}\sum_{n=1}^{L}\exp\left(j2\pi\frac{\kappa n}{N}\right) \sim \frac{L}{N} \cdot \operatorname{si}\left(\pi\kappa\frac{L}{N}\right). \tag{26}$$

The subcarrier distance $|\kappa|$ where the normalized correlation drops down to a value below 0.5 can be estimated by

$$K_c = \left|\operatorname{si}^{-1}(0.5)\right| \cdot \frac{N}{\pi L} \approx 0.2\frac{N}{L}, \tag{27}$$

K_c can be interpreted as a delimiter of the region around any subcarrier at position k where the power of the interference is highly correlated; we thus denote it as *interference correlation range*. The distance grows inversely proportional with the channel length L; a short channel length thus results in a high correlation of the interference. We will see later that the correlation of the interference supports a simplified CFO compensation process, which yields an improved error performance.

Further, it has to be considered that the interference contained in the term $\mathbf{Vx}$ from (17) is constituted of two different types, which affect the signal conditions at subcarrier position k differently. In particular, we encounter self-interference stemming from the signal at subcarrier k itself, which is represented by the diagonal elements in $\mathbf{V}$, and ICI-like distortion stemming from all other subcarrier signals, which is represented by the off-diagonal elements of $\mathbf{V}$. As the transmit symbols in $\mathbf{x}$ are assumed i.i.d., the ICI can be assumed to be uncorrelated with the signal at subcarrier k, and hence the distortion effect due to the ICI can be considered similar to the one of additive white Gaussian noise (AWGN). The self-interference, however, may be strongly correlated with the signal at subcarrier k and thus may directly influence its signal level in a deterministic fashion. However, in the appendix it is shown that the

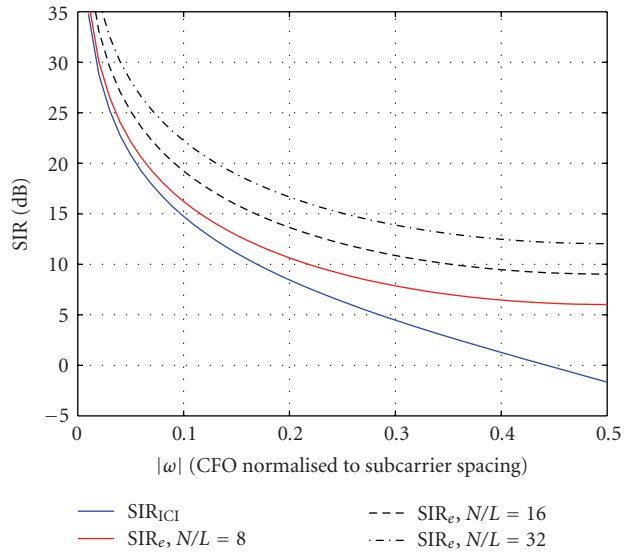

Figure 1: SIR conditions for uncompensated CFO (12) and compensated CFO (28) based on the signal model in (17).

influence of the deterministic distortion evoked by the self-interference is negligible if $L \ll N$ holds, and consequently we may consider the total interference from $\mathbf{Vx}$ as pure ICI-like distortion here.

The power of the useful signal per subcarrier amounts to P_s. Thus, a closed form expression for a lower bound of the SIR resulting from the error matrix $\mathbf{\Gamma}$ can finally be given as

$$\mathrm{SIR}_e = \frac{P_s}{P_i(\omega)} \geq \frac{N}{2L \cdot \sin^2(\pi\omega)}. \tag{28}$$

We observe that an increasing channel length L decreases the SIR proportionally. As the proposed CFO compensation process ignores the error $\mathbf{\Gamma}$, we will not be able to overcome this SIR bound, even if the distortion measures $\overline{\mathbf{\Lambda}}$ and $\mathbf{U}$ needed for the compensation process are estimated perfectly.

To illustrate the obtained results, Figure 1 compares the SIR bound for an uncompensated CFO from (12) with the SIR bound (28) achievable after applying the simplified CFO compensation process. The amount of interference power that can be removed by the suggested process corresponds to $\Delta P_i = \mathrm{SIR}_{\mathrm{ICI}}^{-1} - \mathrm{SIR}_e^{-1}$. If $L = 0$, the interference can be removed completely by the CFO compensation process. For increasing L, however, an increasing share of the interference power is contained in the term $\mathbf{Vx}$ in (17), remaining in the system after compensation. If we set $\Delta P_i = 0$ and solve for L, we obtain the channel length where the compensation process is not capable of providing any gain. The minimum value for this length L is obtained for $|\omega| \to 0$, yielding $N/6$. This means that if $L > N/6$, the gains delivered by the CFO compensation process become vanishingly small, so that its application will no longer be suitable. In Figure 1, this can be observed as the SIR_e curves approach the $\mathrm{SIR}_{\mathrm{ICI}}$ curve for decreasing values of N/L. For $N/L = 8$, the SIR gains achieved after compensation for small CFOs $|\omega| < 0.2$ have become already very small.

3.4. CFO Compensation after Channel Equalization. We focus now in more detail on the CFO compensation process based on the signal model (17), which is carried out after channel equalization by multiplying the equalized signal vector $\hat{\mathbf{y}} = \overline{\mathbf{\Lambda}}^{-1}\mathbf{y}$ with the Hermitian matrix $\mathbf{U}^H$ (note that matrix $\mathbf{U}$ has unitary property). This latter operation represents a convolution of the subcarrier signals in $\hat{\mathbf{y}}$ with $u^*(-\kappa)$, which is given in (10). As the amplitude $u(\kappa)$ drops with $1/\kappa$, it may be sufficient to consider only the subcarriers in closest vicinity to the subcarrier k within the convolution process, which would simplify the entire process significantly. Let the vicinity range of subcarriers, therefore, be limited to K, that is, $|\kappa| \leq K$. The convolution operation can then be specified by

$$\hat{x}_j = \sum_{\kappa=-K}^{K} u^*(\kappa) \cdot \hat{y}_{j+\kappa}, \tag{29}$$

where $\hat{y}_k$ is the kth symbol of vector $\hat{\mathbf{y}}$, and $\hat{x}_j$ is the jth subcarrier signal obtained after equalization and CFO compensation.

To specify a suitable value for the delimiter K, note that $\hat{\mathbf{y}}$ is distorted by interference from $\mathbf{Vx}$, which is strongly correlated over the interference correlation range $|\kappa| \leq K_c$ specified in (27). Furthermore, note that $u(\kappa)$ given in (10) is near to being point-symmetric, that is, $u(-\kappa) \approx -u(\kappa)$ holds. This near point-symmetric property of $u(\kappa)$ results in the fact that the correlated interference affecting the subcarrier signals in close vicinity of subcarrier j is canceled out almost completely in (29). For that reason, it seems to be reasonable to set the delimiter $K = [K_c]$, where $[x]$ denotes the integer nearest to x. Interestingly, simulation results presented in Section 5 show that we are able to achieve a slight performance improvement with this selection compared to the full CFO compensation, where the interference from the total N subcarrier signals is taken into account.

Note that CFO compensation according to (29) can be realized with comparatively small demands on system complexity. Firstly, for practical system setups, K can be limited to small values. Furthermore, $u(\kappa)$ in (10) exhibits a single complex factor independent of κ, which represents the CPE. Compensation of the CPE can be incorporated into the channel equalization process. Therefore, (29) reduces to a convolution with a simple, strictly real-valued function.

4. SIR Analysis in OFDM-SDMA System

Recall the OFDM-SDMA transmission equation from (6). If we want to equalize the effective channel $\mathbf{H}_C$ completely, the only viable approach based on linear techniques is to invert the entire channel matrix $\mathbf{H}_C$—which relates to the approach for OFDMA systems conducted in [18, 19]. However, this matrix is of dimension $MN \times QN$, and hence the complexity of this approach will quickly become infeasible for practical realizations. Although complexity can be reduced by exploiting the block-diagonal band structure of this matrix, it still remains considerably high. Moreover, as CFOs induce phase rotations of the effective subcarrier channels over time, the

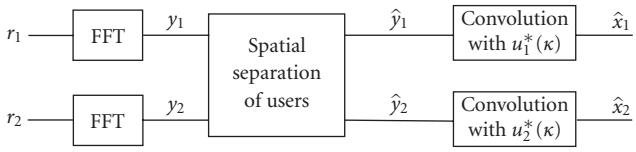

Figure 2: Receiver processing for simplified signal reconstruction with CFO compensation in the SDMA uplink.

matrix $\mathbf{H}_C$ changes every OFDM symbol and thus has to be recomputed frequently, which increases the complexity for the inversion-based compensation even further.

An equalization approach that maintains the subcarrier-wise signal processing for the equalization and thus requires low complexity demands can be enabled if we alternatively adopt the signal model (17) derived in Section 3.2. Herewith, the compound channel $\mathbf{H}_C$ can be written in the structured form:

$$\mathbf{H}_C = \begin{pmatrix} \overline{\mathbf{\Lambda}}_{11} & \overline{\mathbf{\Lambda}}_{12} \\ \vdots & \vdots \\ \overline{\mathbf{\Lambda}}_{M1} & \overline{\mathbf{\Lambda}}_{M2} \end{pmatrix} \cdot \begin{pmatrix} \mathbf{U}_1 & \mathbf{0} \\ \mathbf{0} & \mathbf{U}_2 \end{pmatrix} + \begin{pmatrix} \mathbf{V}_{11} & \mathbf{V}_{12} \\ \vdots & \vdots \\ \mathbf{V}_{M1} & \mathbf{V}_{M2} \end{pmatrix}. \quad (30)$$

The OFDM-SDMA transmission equation then yields

$$\overline{\mathbf{y}} = (\mathbf{\Lambda}_C \cdot \mathbf{U}_C + \mathbf{V}_C)\overline{\mathbf{x}}, \quad (31)$$

where $\mathbf{\Lambda_C}$, $\mathbf{U}_C$, and $\mathbf{V}_C$ are the matrices constituting the compound channel matrix $\mathbf{H}_C$ above. Evidently, this notation enables the two-step equalization process introduced in the previous section. We first equalize the channel contained in matrix $\mathbf{\Lambda}_C$ by a subcarrier-wise equalization of the flat-fading SDMA channel and thereby spatially separate the single user signals. The separated user signals may then be compensated individually for their CFO distortions $\mathbf{U}_q$ as described in Section 3.4. The entire receiver processing for the simplified CFO compensation in the SDMA system is illustrated in Figure 2.

In what follows, we will analyze how the CFO-induced interference will affect spatial diversity gains that can be achieved with a linear multiantenna receiver. As there is some correlation between signal and interference channels, distortion effects from the interference can no longer be expected to be similar to the one of AWGN. In particular, we will analyze the degree of correlation between the channel of the useful signal and the interference channels and derive SIR bounds describing the equivalent situation for AWGN. Analysis will be carried out for the case of no CFO compensation and compensation according to the proposed scheme separately.

4.1. Spatial Diversity Gain. In a brief intermezzo, we derive the basic relations concerning spatial diversity gains that are achievable with linear receivers in case of correlated signals. These relations form the basis for the analysis of the signal conditions in CFO-distorted OFDM-SDMA systems, which will be performed in the succeeding subsections. In particular, we examine here how interference that propagates via a correlated channel will affect the signal conditions at a multiantenna receiver providing spatial diversity gain μ. Following the notion from [34], the spatial diversity gain can be illustrated by assuming a maximum ratio combining (MRC) receiver that combines the signals from μ independent receive antennas. Assume a signal x_1 with mean power P_s, which is transmitted via μ independent Rayleigh-fading channels h_{m1}, $m \in \{1, \ldots, \mu\}$ with unit mean power. At each receiving antenna m, the signal is distorted by AWGN with power N_0. MRC operation then yields a post-MRC signal-to-noise ratio (SNR) of $\mu P_s/N_0$. The SNR thus is increased by factor μ compared to the SNR of the signal at a single receive antenna.

Instead of AWGN, we consider an interfering signal x_2 with mean power N_0 now. The signal at mth receive antenna reads

$$y_m = h_{m1}x_1 + h_{m2}x_2. \quad (32)$$

Let the two signal x_q be uncorrelated, while some correlation between the two channels h_{mq} is assumed. Both variables h_{mq} are assumed to be zero-mean Gaussian variables with variance $var\,(h_{mq}) = E\{h_{mq}^* h_{mq}\}$. The correlation between both variables can be characterized by the correlation coefficient defined as [35]

$$\rho = \frac{\mathrm{cov}(h_{m1}, h_{m2})}{\sqrt{\mathrm{var}(h_{m1})\mathrm{var}(h_{m2})}}, \quad \rho \in [0, 1], \quad (33)$$

where $\mathrm{cov}(h_{m1}, h_{m2})$ stands for the covariance of the two variables given in the parentheses. According to [35, Theorem 10.1], the distribution of h_{m2} conditioned on h_{m1} can be characterized by the two measures:

$$\begin{aligned} E\{h_{m2} \mid h_{m1}\} &= \rho\sqrt{\frac{\mathrm{var}(h_{m2})}{\mathrm{var}(h_{m1})}}h_{m1}, \\ \mathrm{var}(h_{m2} \mid h_{m1}) &= (1-\rho^2)\mathrm{var}(h_{m2}). \end{aligned} \quad (34)$$

Accordingly, h_{m2} can be rewritten as

$$h_{m2} = \rho\sqrt{\frac{\mathrm{var}(h_{m2})}{\mathrm{var}(h_{m1})}}\, h_{m1} + \sqrt{(1-\rho^2)\ \mathrm{var}(h_{m2})}\, z_m, \quad (35)$$

where we introduced a new Gaussian variable z_m with zero mean and unit power, which is independent of h_{m1}. Substituting this equation in (32) yields

$$\begin{aligned} y_m = \underbrace{h_{m1}x_1}_{s} + \underbrace{\rho\sqrt{\frac{\mathrm{var}(h_{m2})}{\mathrm{var}(h_{m1})}}\, h_{m1}x_2}_{f_1} \\ + \underbrace{\sqrt{(1-\rho^2)\ \mathrm{var}(h_{m2})}\, z_m \cdot x_2}_{f_2}. \end{aligned} \quad (36)$$

MRC operation delivering the spatial diversity gain is carried out by multiplying each received signal y_m with the conjugate channel seen by the useful signal x_1 and summing up the signals over all μ receive antennas: $y^{\mathrm{MRC}} = \sum_{m=1}^{\mu} h_{m1}^* y_m$. Within this summation, the signal portions from the first two

components in (36), s and f_1, which both depend on h_{m1}, add up constructively, yielding a mean power of

$$\begin{aligned}\mu^2 E\{ss^*\} &= \mu^2 \ \mathrm{var}(h_{m1})P_s,\\ \mu^2 E\{f_1 f_1^*\} &= \mu^2\rho^2 \ \mathrm{var}(h_{m2})N_0\end{aligned} \tag{37}$$

after MRC operation. In contrast to that, the signal portions from the third component in (36), f_2, add up with arbitrary phase, so that the mean power for these signal portions yields after MRC

$$\mu E\{f_2 f_2^*\} = \mu(1-\rho^2)\mathrm{var}(h_{m2})N_0. \tag{38}$$

Now let, for simplicity, $\mathrm{var}(h_{m1}) = \mathrm{var}(h_{m2}) = 1$. With the aforementioned results, we obtain for the post-MRC SIR

$$\mathrm{SIR}^{\mathrm{MRC}} = \frac{\mu P_s}{[(\mu-1)\rho^2+1]N_0} = \nu\cdot\mu\frac{P_s}{N_0}, \tag{39}$$

clearly revealing that the spatial diversity gain factor μ is diminished by

$$\nu = [(\mu-1)\rho^2+1]^{-1} < 1. \tag{40}$$

Thus, ν represents the effective SNR loss factor owing to the channel correlation $\rho > 0$.

4.2. No Compensation of CFO Distortions. Now we turn our focus back on the signal conditions in the OFDM-SDMA system in case the ICI distortions are not compensated. Consider the signal received at antenna m, which, according to (6), is given as

$$\mathbf{y}_m = \mathbf{U}_1\mathbf{\Lambda}_{m1}\mathbf{x}_1 + \mathbf{U}_2\mathbf{\Lambda}_{m2}\mathbf{x}_2. \tag{41}$$

In case all subcarriers carry signals with identical transmit power, the statistical properties of the ICI are identical for all the elements contained in $\mathbf{y}_m$. Therefore, we carry out the analysis exemplarily for the first element of vector $\mathbf{y}_m$, denoted as y_m. To separate the ICI from the useful signal, we define $\overline{\mathbf{u}}_q$ as the first row vector of matrix $\mathbf{U}_q$, where the first element has been replaced by zero. The transmission equation then yields

$$y_m = u(0)(\lambda_{m1}x_1 + \lambda_{m2}x_2) + \underbrace{\overline{\mathbf{u}}_1\mathbf{\Lambda}_{m1}\mathbf{x}_1 + \overline{\mathbf{u}}_2\mathbf{\Lambda}_{m2}\mathbf{x}_2}_{\mathrm{ICI}}, \tag{42}$$

where λ_{mq} is the channel coefficient for the first subcarrier extracted from matrix $\mathbf{\Lambda}_{mq}$, and x_q is the transmit signal of user q at the first subcarrier. We set x_1 as the useful signal. An appropriate equalizer is able to remove the signal portion $\lambda_{m2}x_2$ if estimates of the channels λ_{mq} can be obtained with sufficient quality. The two scalar products within (42), however, will remain in the system as ICI. The signal structure in the aforementioned equation is now similar to (32), and hence we can use the results from the preceding subsection to determine achievable spatial diversity gains here. Clearly, the two scalar products representing the ICI in (42) are constituted of multiple interfering signals. However, as all elements within vector $\mathbf{x}_q$ are assumed i.i.d., each scalar product can be modeled by a single random variable, whose power is constituted from the sum of powers from the single elements in $\overline{\mathbf{u}}_q\mathbf{\Lambda}_{mq} =: \mathbf{f}_q$. In particular, we yield for the power of the interfering channel:

$$E\left\{\mathbf{f}_q\mathbf{f}_q^H\right\} = E\left\{\overline{\mathbf{u}}_q\mathbf{\Lambda}_{mq}\mathbf{\Lambda}_{mq}^H\overline{\mathbf{u}}_q^H\right\} = \sum_{j=1}^{N-1}|u(j)|^2 \le 1 - \mathrm{si}^2\left(\pi\omega_q\right), \tag{43}$$

where we used the upper bound for P_{ICI} presented in Section 3.1. The covariance between the useful channel λ_{m1} and the interference channels $\overline{\mathbf{u}}_q\mathbf{\Lambda}_{mq}$ is determined by

$$\mathbf{z}_q = E\left\{\lambda_{m1}^*\overline{\mathbf{u}}_q\mathbf{\Lambda}_{mq}\right\}. \tag{44}$$

As channels from different users are assumed uncorrelated, $\mathbf{z}_q$ yields a vector with nonzero entries for $q = 1$ only. The N elements of the covariance vector $\mathbf{z}_1$ can be characterized by the function

$$z(\kappa) = \begin{cases}0, & \kappa = 0,\\ u(\kappa)\cdot r(\kappa), & \kappa\in\{1,\ldots,N-1\},\end{cases} \tag{45}$$

with $r(\kappa)$ being the subcarrier correlation function defined in Section 2.3. The total power of the covariance vector $\mathbf{z}_1$ is determined as

$$\mathbf{z}_1^H\mathbf{z}_1 = \sum_{\kappa=1}^{N-1}|u(\kappa)|^2|r(\kappa)|^2, \tag{46}$$

which can be read as the power of the covariance $|\mathrm{cov}|^2$ of an equivalent random process based on a single random variable. With these results, we can determine a measure representing the correlation between the useful channel and the sum of interference channels, which is calculated equivalently to the correlation coefficient in (33):

$$\rho^2 = \frac{\mathbf{z}_1^H\mathbf{z}_1}{E\{\lambda_{m1}^*\lambda_{m1}\}E\left\{\mathbf{f}_1\mathbf{f}_1^H\right\}} \ge \frac{\sum_{\kappa=1}^{N-1}|u(\kappa)|^2|r(\kappa)|^2}{1-\ \mathrm{si}^2(\pi\omega_1)}. \tag{47}$$

Evaluating this measure for varying L reveals that $\rho^2 \approx 1$ for $L \ll N$, suggesting that the useful channel and the interference channels for the ICI generated from $\mathbf{x}_1$ are nearly fully correlated. Evidently, this results mainly from the high-frequency correlation of subcarrier channels that is valid for $L \ll N$.

Consequently, we can conclude here that if an MRC-like signal combination is performed at the multiantenna receiver, not only the signal portions of the useful signal x_1 but also the ones of the interference from $\mathbf{x}_1$ will add up fully coherently. In contrast to that, there is no correlation between the useful channel λ_{m1} and the interference channels $\overline{\mathbf{u}}_q\mathbf{\Lambda}_{mq}$, $q \ne 1$, as the covariance of the corresponding channels yields zero. Consequently, this distortion will behave similarly to AWGN. Resorting to the derivation of the SIR in (39) in the preceding section, we yield for the achievable SIR in an OFDM-SDMA system with spatial diversity gain μ:

$$\mathrm{SIR}_{\mathrm{ICI}}^{\mathrm{MRC}} \ge \frac{\mu\mathrm{si}^2(\pi\omega_1)}{\mu\left(1-\mathrm{si}^2(\pi\omega_1)\right)+\left(1-\mathrm{si}^2(\pi\omega_2)\right)}, \tag{48}$$

where we have used the bounds for P_u and P_{ICI} from Section 3.1 for the total power of useful signal and ICI, respectively. This result shows that in the OFDM-SDMA system with diversity gain μ, the ICI power generated by any user $q \neq 1$ is effectively attenuated by factor μ (i.e., the diversity gain can be realized completely), while the ICI generated from the CFO of user $q = 1$ himself is fully preserved (i.e., no diversity gain is achievable). If all users Q have a CFO of the same size, $\omega_q = \omega$ for all q, then the effective reception SIR (referring to the mean power of each user's signal measured at any receive antenna m) for the equivalent AWGN case can be given as

$$\mathrm{SIR}_{\mathrm{ICI}} \geq [\mu + Q - 1]^{-1} \frac{\mathrm{si}^2(\pi\omega)}{1 - \mathrm{si}^2(\pi\omega)}. \tag{49}$$

This result is equivalent to the SIR bound for the single-antenna case (12), reduced by the effective SIR-loss factor $\eta = [\mu + Q - 1]^{-1}$.

4.3. Compensation of CFO Distortions. Next we consider the case where the CFO distortions are compensated according to the proposed concept. Then interference results from the signal components contained in matrix $\mathbf{V}_C$ in (31) only, and the signal received at antenna m reads

$$\mathbf{y}_m = \overline{\mathbf{\Lambda}}_{m1}\mathbf{U}_1\mathbf{x}_1 + \overline{\mathbf{\Lambda}}_{m2}\mathbf{U}_2\mathbf{x}_2 + \mathbf{V}_{m1}\mathbf{x}_1 + \mathbf{V}_{m2}\mathbf{x}_2. \tag{50}$$

Again, we define $\mathbf{x}_1$ as the useful signal. The proposed equalization and ICI compensation concept removes the interference from $\overline{\mathbf{\Lambda}}_{m2}\mathbf{U}_2\mathbf{x}_2$ as well as the the ICI induced by $\mathbf{U}_1$, and correspondingly solely the interference from $\mathbf{V}_{mq}\mathbf{x}_q$ remains in the system. Equivalently to the analysis carried out in the preceding subsection, we will now determine the correlation between useful channels and the channels of the residual interference to specify achievable spatial diversity gains. However, to ease analysis here, we initially focus on the entire channel matrices $\overline{\mathbf{\Lambda}}_{m1}$ and $\mathbf{V}_{mq}$ to specify the overall statistical properties. Afterwards, we determine the signal conditions per subcarrier signal by averaging over the total N subcarriers of the system.

The mean power of the interfering channel $\mathbf{V}_{mq}$ per subcarrier amounts to

$$\frac{1}{N}\,\mathrm{tr}\left(E\left\{\mathbf{V}_{mq}^H\mathbf{V}_{mq}\right\}\right) \leq \frac{L}{N}\cdot 2\sin^2\left(\pi\omega_q\right). \tag{51}$$

For the bound, we used the result from (23). Correspondingly, the mean power of the useful channel $\overline{\mathbf{\Lambda}}_{m1}$ yields

$$\frac{1}{N}\,\mathrm{tr}\left(E\left\{\overline{\mathbf{\Lambda}}_{m1}^H\overline{\mathbf{\Lambda}}_{m1}\right\}\right) = \frac{1}{N}\,\mathrm{tr}(\mathbf{I}) = 1. \tag{52}$$

The covariance between useful channel and interfering channel can be characterized by the covariance matrix:

$$\mathbf{Z}_q = E\left\{\overline{\mathbf{\Lambda}}_{m1}^H\mathbf{V}_{mq}\right\}. \tag{53}$$

As $\mathbf{V}_{mq}$ is constituted of the channel coefficients related to channel $\overline{\mathbf{\Lambda}}_{mq}$, the covariance matrix $\mathbf{Z}_q$ will have nonzero entries for $q = 1$ only. The corresponding matrix $\mathbf{Z}_1$ can be determined as follows. Using the definitions of $\overline{\mathbf{\Lambda}}$ from (14) and $\mathbf{V}$ from (17), $\overline{\mathbf{\Lambda}}_{m1}^H\mathbf{V}_{m1}$ can be written as $(\mathbf{F}\mathbf{P}_1^H\overline{\mathbf{H}}_{m1}^H\mathbf{P}_2^H)(\mathbf{P}_2\overline{\mathbf{H}}_{m1}\mathbf{\Gamma}_1\mathbf{F})$. For the moment we will exclude the outer DFT matrices $\mathbf{F}$ and determine the expectation value of the inner matrix product. $\mathbf{P}_1^H\overline{\mathbf{H}}_{m1}^H\mathbf{P}_2^H$ is a circular Toeplitz matrix based on the channel impulse response $\overline{h}_l$, and $\mathbf{P}_2\overline{\mathbf{H}}_{m1}\mathbf{\Gamma}_1$ was shown in Section 3.2 to be a matrix with zero entries except for the submatrix $\mathbf{V}_u$ found in its upper right corner. The expectation value of the product of these two components thus yields a matrix with zero entries except for the $L\times L$ antidiagonal submatrix in its upper-right corner, whose L antidiagonal elements ξ_i represent partial sums of the channel power weighted by γ_{-i}:

$$\xi_i = \gamma_{-i}\sum_{l=i}^{L}\sigma_l^2\,, \qquad i \in \{1,\ldots,L\} \tag{54}$$

with γ_n defined in (16). From the covariance matrix, we can determine the mean power of the covariance between useful and interfering channels per subcarrier signal according to

$$\begin{aligned}\frac{1}{N}\mathrm{tr}\left(\mathbf{Z}_1\mathbf{Z}_1{}^H\right) &= \sum_{i=1}^{L}|\xi_i|^2 \\ &\leq |\gamma_n|^2\frac{1}{(L+1)^2}\sum_{i=1}^{L}i^2 \\ &= |\gamma_n|^2\frac{L(2L+1)}{6(L+1)},\end{aligned} \tag{55}$$

where the upper bound is obtained for a uniform PDP. Note that $|\gamma_n|^2 = 4\sin^2(\pi\omega_1)$. Similar to (47), we can now determine a measure equivalent to the squared correlation coefficient:

$$\begin{aligned}\rho^2 &= \frac{N^{-1}\,\mathrm{tr}\left(\mathbf{Z}_1\mathbf{Z}_1{}^H\right)}{N^{-1}\,\mathrm{tr}\left(E\left\{\overline{\mathbf{\Lambda}}_{m1}^H\overline{\mathbf{\Lambda}}_{m1}\right\}\right)N^{-1}\,\mathrm{tr}\left(E\left\{\mathbf{V}_{m1}^H\mathbf{V}_{m1}\right\}\right)} \\ &\approx \frac{2L+1}{3(L+1)} \\ &< \frac{2}{3}.\end{aligned} \tag{56}$$

Assuming again a receiver with spatial diversity gain μ, we may now determine the SIR for the useful signal after an MRC-like signal combination over μ independent observations. Resorting to the derivation of the SIR in (39), we yield for the interference from $\mathbf{V}_{m1}\mathbf{x}_1$ a mean power of $\mu\nu^{-1}P_i(\omega_1)$, with the interference power $P_i(\omega)$ according to (25) and the SIR loss factor ν from (39). As all other interference channels $\mathbf{V}_{mq}$, $q \neq 1$, are uncorrelated with the useful channel $\overline{\mathbf{\Lambda}}_{m1}$, the corresponding interference $\mathbf{V}_{mq}\mathbf{x}_q$ adds up incoherently, yielding a mean power of $\mu P_i(\omega_2)$. Hence, we obtain the post-MRC SIR

$$\mathrm{SIR}_e^{\mathrm{MRC}} = \frac{\mu P_s}{\nu^{-1}P_i(\omega_1) + P_i(\omega_2)}. \tag{57}$$

If we have multiple users Q who all have a constant CFO, that is, $\omega_q = \omega$ for all q, the effective reception SIR at any antenna m for the equivalent AWGN case can be bounded by

$$\mathrm{SIR}_e \geq [(\mu-1)\rho^2 + Q]^{-1} \frac{N}{2L\sin^2(\pi\omega)}, \tag{58}$$

where we used the bound for $P_i(\omega)$ from (25), and ρ^2 should be used as specified in (56). This expression is equivalent to the SIR bound found for the single-antenna case in (28) reduced by the effective SIR-loss factor $\eta_e = [(\mu-1)\rho^2+Q]^{-1}$. Note here that the CFO-induced interference scales with the number of parallel SDMA users Q. In case of full correlation ($\rho = 1$), the SIR-loss factor η_e is identical to η, the factor found in case of no CFO compensation in (49). As a major result, we conclude here that the correlated interference from the CFO distortion results in an increase of the effective SIR-loss if a receiver with spatial diversity gain $\mu > 1$ is employed.

5. Simulation Results

In this section we will provide numerical simulations to verify our analytical results found in the previous sections. For the simulations, we assume OFDM signal transmission via a noisy channel, that is, the transmission equation (6) is now given by

$$\overline{\mathbf{y}} = \mathbf{H}_C \cdot \overline{\mathbf{x}} + \mathbf{n}, \tag{59}$$

where $\mathbf{n}$ is a vector consisting of MN AWGN samples with power N_0. Thus, the mean reception SNR amounts to P_s/N_0 for the signal of any user at any receive antenna. As we have indicated that the CFO-induced interference can be expected to behave like AWGN, it can be assumed that this interference degrades the interference-free AWGN performance (i.e., no CFO is present) according to the amount of interference power. In particular, if the SNR P_s/N_0 is equal to the CFO-induced SIR, we can expect that the transmission experiences a performance degradation of 3 dB compared to the interference-free case. (As interference and AWGN are assumed to be independent, their joint distortion can be considered as Gaussian-like with power equal to the sum of powers from the two independent processes.) This basic principle will be used to verify the SIR bounds derived in the preceding sections.

We consider an OFDM-SDMA system with $N = 64$ subcarriers, where $Q = 2$ single-antenna user terminals are granted simultaneous access. For the bounds to be tight, all N subcarriers are occupied with transmission symbols from both users. The channel between each antenna link is modeled as Rayleigh-fading with $L + 1 = 5$ channel taps and a uniform PDP. The normalized CFO is fixed to $\omega = 0.1$. As a performance measure, we use the bit-error rate (BER) that is achieved for an uncoded transmission of uncorrelated 16QAM symbols, averaged over both users. We use a zero forcing (ZF) equalizer to equalize the channel distortions and spatially separate the user signals per subcarrier. The diagonal channel $\mathbf{\Lambda}_C$ from (31) as well as the CFOs ω_q are assumed to be known perfectly at the receiver.

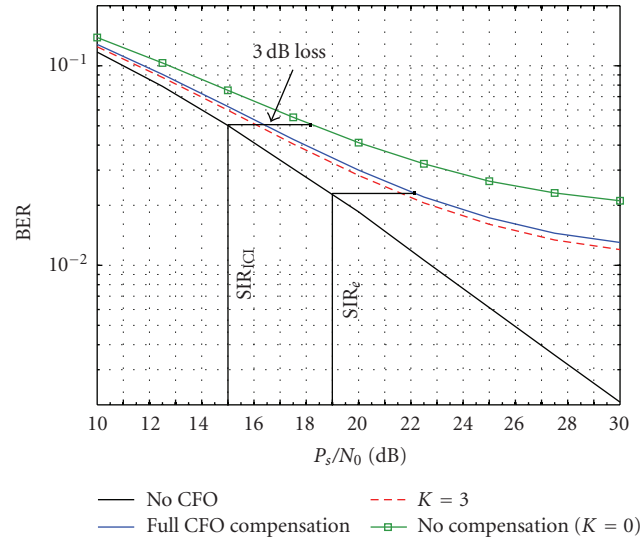

Figure 3: BER performance of SISO system distorted by normalized CFO $\omega = 0.1$.

Based on the signal model (17), we first examine the achievable performance for a single-antenna link (SISO). Results are given in Figure 3. The solid bold line shows the achievable BER performance in case no CFO is present. The suggested compensation approach shows a significantly degraded performance. At an SNR P_s/N_0 equal to the SIR bound (28), which amounts to 19 dB for the given parameter setting, it clearly exhibits a performance loss of 3 dB. This observation thus verifies the bound derived in (28).

The performance curve of the CFO compensated system runs into an error floor for high SNR that corresponds to the BER performance achievable with the CFO-free performance at about 22 dB—which is about 3 dB higher than the SIR bound. The reason for that can be found in the distribution of the interference generated from the distortion terms in $\mathbf{Vx}$ in (17). Note that the values in $\mathbf{Vx}$ are generated from products of the independent random variables $\overline{h}_l$ in $\mathbf{V}$ and the data symbols in $\mathbf{x}$, which are all assumed to be Gaussian. The resulting distribution function for the values in $\mathbf{Vx}$ is thus in general no longer Gaussian. Instead, we observe that the majority of the values from this distribution is much more concentrated around their mean than in the Gaussian case. Due to this fact, the achieved error floor is significantly lower than it would be if the interference behaved like Gaussian noise with identical power. However, it is worth noting that with increasing L and thus with an increasing number of independent variables $\overline{h}_l$ in $\mathbf{V}$, the distribution of the values in $\mathbf{Vx}$ approaches the Gaussian case—thanks to the central limit theorem.

If we apply the CFO compensation technique that removes the ICI from the subcarriers in close vicinity $\kappa \leq K$ only (see Section 3.4), we obtain the performance given by the dashed line for $K = [K_c] = 3$. Interestingly, for the choice of K according to K_c given in (27), the CFO compensation accounting only for some of the ICI distortion achieves a slight performance improvement compared to the

full CFO compensation. Obviously, this is a benefit related to the correlated interference from $\mathbf{Vx}$ in (17), as detailed in Section 3.4.

If we do not compensate for the ICI caused by the CFO but compensate for the CPE only, which corresponds to the case of applying the compensator (29) with $K = 0$, we obtain the performance represented by the uppermost curve. For an SNR equal to the bound in (12), which amounts to 15 dB for the given parameter setting, we clearly observe a performance loss of 3 dB compared to the performance where no CFO is present.

For the 2-user SDMA case, we consider ZF equalization to separate the signals of the different users. In [34] the diversity gain delivered by the ZF receiver has been shown to yield $\mu = M - Q + 1$. For our examinations, we consider two cases: a receiver with $M = 2$ and $M = 3$ antennas, providing a diversity gain of $\mu = 1$ and $\mu = 2$, respectively. Performance results are shown in Figure 4. The dashed curves refer to $\mu = 1$, while the solid curves refer to $\mu = 2$. The curves representing full CFO compensation according to the proposed scheme exhibit a 3 dB performance loss at an SNR equal to the SIR from (58) compared to the curve of CFO-free transmission, which amounts to 16 dB for $\mu = 1$ and 15 dB for $\mu = 2$, respectively, for the given parameter setting. These losses are highlighted in Figure 4 by the horizontal black lines, clearly verifying the bound derived in (58). As in the SISO case, we observe that we can achieve a slight performance improvement if we use the simplified CFO compensation process based on (29) with $K = 3$. In case we do not compensate the ICI caused by the CFO, we achieve a severely degraded performance, which clearly exhibits a 3 dB performance loss at an SNR of 12 dB for $\mu = 1$ and 10 dB for $\mu = 2$, respectively, corresponding to the analytical bound (49).

In Figure 5 we examine the behavior of the BER when the CFO compensation process based on (29) is applied for different values of the delimiter K. We focus on a constant SNR $P_s/N_0 = 20$ dB, which reflects the BER of the error floor for $\mu = 1$. For the selected values of N/L, the subcarrier correlation range K_c from (27) amounts to 3.2 and 1.6, respectively. Interestingly, the corresponding curves exhibit their minimum at $K = 3$ and $K = 2$, respectively, which is the nearest integer to K_c. Hence, selecting $K = [K_c]$ indeed seems to be a good choice. This result leads us to the conclusion that it definitely suffices to consider only the subcarrier signals in closest vicinity within the CFO compensation via (29).

To illustrate the performance degradation caused by the incomplete compensation of the CFO effects in the OFDM-SDMA system, we specify the effective SNR loss ΔSNR based on the ratio of the interference power bound from (58) and the AWGN power N_0 as done in [8], which yields (in dB)

$$\Delta\text{SNR} = 10\log_{10}\left(1 + \frac{\eta_e N P_s}{2L\sin^2(\pi\omega)N_0}\right). \quad (60)$$

The numerical evaluation of the effective SNR loss for various CFO sizes ω is depicted versus the SNR P_s/N_0 in Figure 6; the corresponding parameter setting is specified in its caption. In accordance with the observations drawn

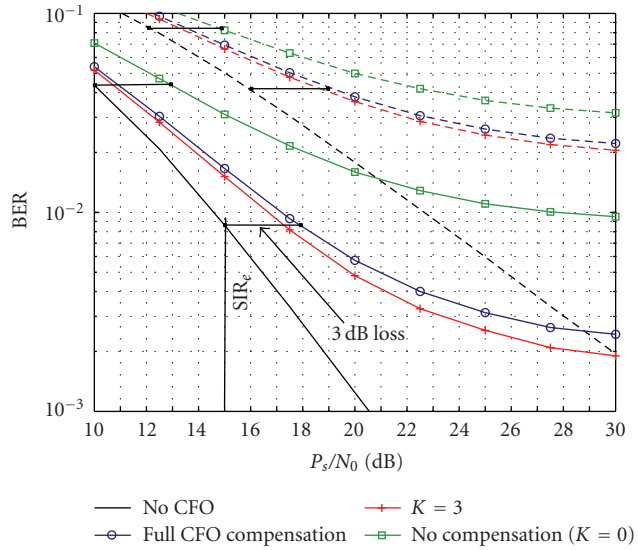

Figure 4: BER performance of 2-user SDMA system distorted by normalized CFO $\omega = 0.1$ with ZF receiver. Dashed line: diversity gain $\mu = 1$. Solid line: $\mu = 2$.

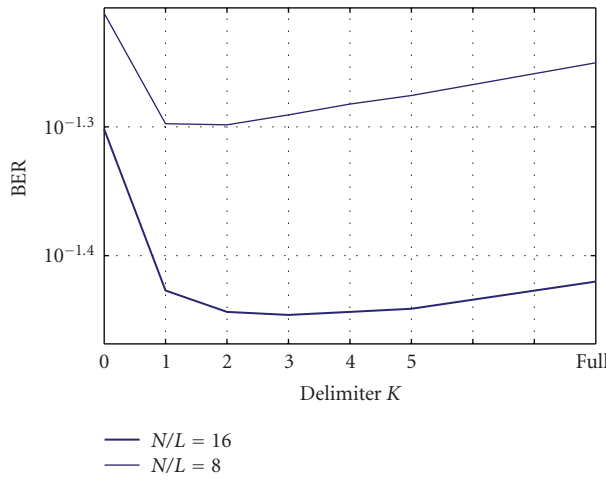

Figure 5: BER performance at SNR = 20 dB versus delimiter K. $\mu = 1$, $Q = 2$, $\omega = 0.1$.

from Figure 4, where evaluations where based on a CFO of size $\omega = 0.1$, the corresponding curve indicates here a 3 dB SNR loss at an SNR $P_s/N_0 = 16$ dB. For comparison, we also added the SNR loss for the case of no ICI compensation (dashed curves), where we used the interference power bound from (49). Although we observe that the proposed CFO compensation is able to reduce the SIR loss significantly, it still increases steeply for increasing CFO size ω. If the CFO amounts to 20% of the subcarrier spacing, the performance of the system is degraded by 3 dB already at an SNR level of about 10 dB.

These results show that the system's sensitivity toward CFO errors is still very high, and hence we conclude that with the suggested approach, we can conveniently compensate CFOs of small size only. Thus, the method is suitable for a

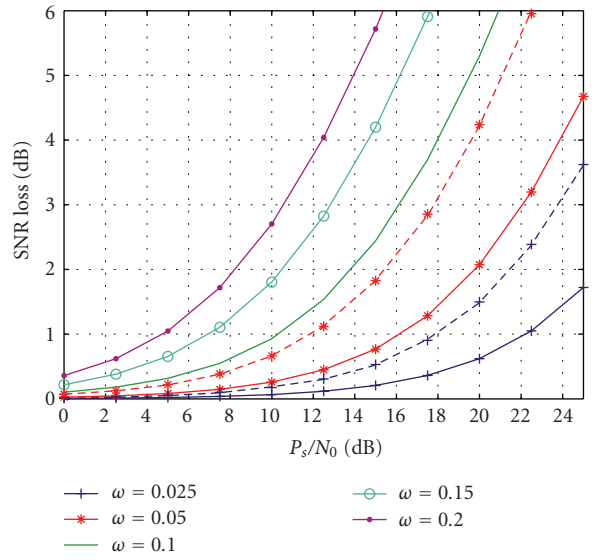

FIGURE 6: SNR loss after CFO compensation versus SNR for CFOs of different size ω. Solid line: ICI compensation. Dashed line: no compensation. $\mu = 1$, $Q = 2$, $N/L = 16$.

fine-frequency synchronization only, and hence it has to rely on a coarse synchronization, which has to be established in advance. In a practical system, such a coarse synchronization can be achieved if the terminals use their frequency estimates obtained during the preceding downlink phase for a proper frequency precompensation of their transmit signals. We denote this as *frequency advance*, which has been the basic concept for our real-time system implementation that has been reported in [30]. It is worth noting that the analysis presented in this paper and in particular the derived bounds for the SIRs served as an important guideline in preparing the experiments that have been summarized in that reference, which have shown that a convenient system operation in a practical setup can be achieved.

Finally, note that if the CFOs are kept small, the signal degradation from ICI is limited, and thus common pilot-based channel estimation techniques can still be used to obtain channel estimates of sufficient quality. The more pilots available in one OFDM symbol can be used for that channel estimation, the better the ICI can be suppressed, as the ICI behaves similar to AWGN. Moreover, the CFOs ω_q of the single users $q \in \{1,\ldots,Q\}$ can be obtained from observing the phase drift of the estimated subcarrier channels λ_k over several successive OFDM symbols. With (10), the ICI coefficients $u(\kappa)$ can then be determined, which can finally be applied in (29) for proper ICI compensation of the single users' signals.

6. Conclusion

We have investigated OFDM-SDMA uplink transmission in the presence of multiple users' CFOs. We modified the common signal model suitably to enable a subcarrier-wise SDMA equalization followed by a user-specific CFO compensation, yielding a simple equalization process ready to be applied in practice. However, as CFOs violate the periodic structure of the OFDM signals, some interference remains in the system after CFO compensation, which cannot be compensated as long as simple frequency domain processing is targeted. The SIR conditions in OFDM-SDMA systems have been analyzed if CFOs are compensated according to the proposed scheme as well as if they are not. We derived suitable upper bounds for the SIRs depending on the system parameters, which have been verified by numerical simulations. To enable a convenient operation of the proposed scheme, we conclude from the results that the users' CFOs should not exceed values that are much larger than a few percent of the OFDM subcarrier spacing, which classifies this scheme as a technique for fine frequency synchronization. Correspondingly, coarse-frequency synchronization has to be ensured, which can easily be established if the CFO estimates from the downlink are used in the uplink for a proper predistortion of each user's transmit signal, as suggested also in [10] and practically realized in [30]. Together with this concept, the proposed scheme can be regarded as a convenient solution to synchronize the OFDM-SDMA uplink. Note that this concept based on coarse synchronization also enables to estimate user channels based on common pilot-based channel estimation techniques. Suitable estimates of the users' CFOs can then be obtained from the phase drift of the estimated channels observed over several consecutive OFDM symbols.

Appendix

A. Correlation between Self-Interference and Useful Signal

To determine the correlation between the self-interference and the useful signal at any subcarrier k, we determine the covariance between the self-interference coefficient (i.e., the kth diagonal element of matrix $\mathbf{V}$) and the channel coefficient λ_k. As indicated earlier, the interference conditions evoked by matrix $\mathbf{V}$ are independent of the actual subcarrier position k, and hence it suffices to determine the covariance at a single subcarrier position; specifically we choose $k = 1$. The channel coefficient is given as $\lambda_1 = \sum_{l=0}^{L} \overline{h}_l$. Denote the first diagonal element of $\mathbf{V}$ as v_{11}. Considering the structure of matrix $\mathbf{V}$ based on the submatrix $\mathbf{V}_u$ (see Section 3.2), v_{11} can be calculated as

$$v_{11} = \frac{1}{N} \sum_{m=0}^{L-1} \sum_{l=m+1}^{L} \gamma_{-l+m} \overline{h}_l. \tag{A.1}$$

As both coefficients λ_1 and u_{11} have an expectation value of zero, the covariance is defined as $\mathrm{cov} = E\{\lambda_1^* v_{11}\}$. With the uniform PDP, we yield for the covariance of the two coefficients

$$\mathrm{cov} = \frac{\gamma_{-1}}{N(L+1)} \sum_{m=1}^{L} \sum_{l=0}^{L-m} \exp(-j\varphi l). \tag{A.2}$$

The second sum term on the right hand side represents a geometric series, so that similarly to (10) the si-function can be used to obtain an approximation, which is given as

$$\sum_{l=0}^{L-m} \exp(-j\varphi l) = \underbrace{\exp\left(-j\pi\omega\frac{L-m}{N}\right)}_{\approx 1} \underbrace{\mathrm{si}\left(\pi\omega\frac{L-m+1}{N}\right)}_{\approx 1} \cdot (L-m). \tag{A.3}$$

As usually $L \ll N$ holds, the exponential function as well as the si-function generate values that are very close to one for any $m \in \{1, \ldots L\}$. Hence, both terms can be upper bounded with constant value one. Herewith the covariance can be upper bounded by

$$\mathrm{cov} < \frac{\gamma_{-1} L}{2N}. \tag{A.4}$$

Assuming the signals λ_1, ν_{11} to be Gaussian, the amount of power P_c devoted to the self-interference can with [35, Theorem 10.1] be determined by

$$P_c = |\mathrm{cov}|^2 \cdot P_s < \frac{L^2}{N^2}\sin^2(\pi\omega) \cdot P_s. \tag{A.5}$$

With this result, we can assess the ratio of the self-interference power to the total interference power $P_i(\omega)$ given in (25), yielding

$$\frac{P_c}{P_i(\omega)} \approx \frac{L}{2N}. \tag{A.6}$$

For $L \ll N$, we conclude that the amount of self-interference is vanishingly small; hence there is no need to consider the self-interference separately to account for its special properties.

References

[1] P. Vandenameele, L. van der Perre, M. G. E. Engels, B. Gyselinckx, and H. J. De Man, "A combined OFDM/SDMA approach," *IEEE Journal on Selected Areas in Communications*, vol. 18, no. 11, pp. 2312–2321, 2000.

[2] X. Cai and G. B. Giannakis, "Bounding performance and suppressing intercarrier interference in wireless mobile OFDM," *IEEE Transactions on Communications*, vol. 51, no. 12, pp. 2047–2056, 2003.

[3] P. Jung and G. Wunder, "On time-variant distortions in multicarrier tansmission with application to frequency offsets and phase noise," *IEEE Transactions on Communications*, vol. 53, no. 9, pp. 1561–1570, 2005.

[4] T. Keller, L. Piazzo, P. Mandarini, and L. Hanzo, "Orthogonal frequency division multiplex synchronization techniques for frequency-selective fading channels," *IEEE Journal on Selected Areas in Communications*, vol. 19, no. 6, pp. 999–1008, 2001.

[5] B. Ai, Z.-X. Yang, C.-Y. Pan, J.-H. Ge, Y. Wang, and Z. Lu, "On the synchronization techniques for wireless OFDM systems," *IEEE Transactions on Broadcasting*, vol. 52, no. 2, pp. 236–244, 2006.

[6] L. Häring and A. Czylwik, "Synchronization in MIMO-OFDM systems," *Advances in Radio Sciences*, vol. 2, pp. 147–153, 2004.

[7] A. M. Tonello, N. Laurenti, and S. Pupolin, "Analysis of the uplink of an asynchronous multi-user DMT OFDMA system impaired by time offsets, frequency offsets, and multi-path fading," in *Proceeding of the 52nd IEEE Vehicular Technology Conference (VTC '00)*, vol. 3, pp. 1094–1099, Boston, Mass, USA, September 2000.

[8] M. S. El-Tanany, Y. Wu, and L. Hazy, "OFDM uplink for interactive broadband wireless: analysis and simulation in the presence of carrier, clock and timing errors," *IEEE Transactions on Broadcasting*, vol. 47, no. 1, pp. 3–19, 2001.

[9] L. Kuang, J. Lu, Z. Ni, and J. Zheng, "Nonpilot-aided carrier frequency tracking for uplink OFDMA systems," in *Proceedings of IEEE International Conference on Communications (ICC '04)*, vol. 6, pp. 3193–3196, Paris, France, June 2004.

[10] M. Morelli, C.-C. Kuo, and M.-O. Pun, "Synchronization techniques for orthogonal frequency division multiple access (OFDMA): a tutorial review," *Proceedings of the IEEE*, vol. 95, no. 7, pp. 1394–1427, 2007.

[11] J.-J. van de Beek, P. O. Börjesson, M.-L. Boucheret, et al., "A time and frequency synchronization scheme for multiuser OFDM," *IEEE Journal on Selected Areas in Communications*, vol. 17, no. 11, pp. 1900–1914, 1999.

[12] H. Bölcskei, "Blind high-resolution uplink synchronization of OFDM-based multiple access schemes," in *Proceedings of the 2nd IEEE Workshop on Signal Processing Advances in Wireless Communications (SPAWC '99)*, pp. 166–169, Annapolis, Md, USA, May 1999.

[13] S. Barbarossa, M. Pompili, and G. B. Giannakis, "Channel-independent synchronization of orthogonal frequency division multiple access systems," *IEEE Journal on Selected Areas in Communications*, vol. 20, no. 2, pp. 474–486, 2002.

[14] Y. Yao and G. B. Giannakis, "Blind carrier frequency offset estimation in SISO, MIMO, and multiuser OFDM systems," *IEEE Transactions on Communications*, vol. 53, no. 1, pp. 173–183, 2005.

[15] Z. Cao, U. Tureli, and Y.-D. Yao, "User separation and frequency-time synchronization for the uplink of interleaved OFDMA," in *Proceedings of the 36th Asilomar Conference on Signals, Systems and Computers*, vol. 2, pp. 1842–1846, Pacific Grove, Calif, USA, November 2002.

[16] M. Morelli, "Timing and frequency synchronization for the uplink of an OFDMA system," *IEEE Transactions on Communications*, vol. 52, no. 2, pp. 296–306, 2004.

[17] M.-O. Pun, M. Morelli, and C.-C. J. Kuo, "Maximum-likelihood synchronization and channel estimation for OFDMA uplink transmissions," *IEEE Transactions on Communications*, vol. 54, no. 4, pp. 726–736, 2006.

[18] Z. Cao, U. Tureli, Y.-D. Yao, and P. Honan, "Frequency synchronization for generalized OFDMA uplink," in *Proceedings of IEEE Global Telecommunications Conference (GLOBECOM '04)*, vol. 2, pp. 1071–1075, Dallas, Tex, USA, November 2004.

[19] C. Ibars and Y. Bar-Ness, "Inter-carrier interference cancellation for OFDM systems with macrodiversity and multiple frequency offsets," *Wireless Personal Communications*, vol. 26, no. 4, pp. 285–304, 2003.

[20] R. Fantacci, D. Marabissi, and S. Papini, "Multiuser interference cancellation receivers for OFDMA uplink communications with carrier frequency offset," in *Proceedings of IEEE Global Telecommunications Conference (GLOBECOM '04)*, vol. 5, pp. 2808–2812, Dallas, Tex, USA, November 2004.

[21] D. Huang and K. B. Letaief, "An interference-cancellation scheme for carrier frequency offsets correction in OFDMA systems," *IEEE Transactions on Communications*, vol. 53, no. 7, pp. 1155–1165, 2005.

[22] W. G. Jeon, K. H. Chang, and Y. S. Cho, "An equalization technique for orthogonal frequency-division multiplexing systems in time-variant multipath channels," *IEEE Transactions on Communications*, vol. 47, no. 1, pp. 27–32, 1999.

[23] C.-Y. Hsu and W.-R. Wu, "Low-complexity CFO compensation for uplink OFDMA systems," in *Proceedings of the 17th IEEE International Symposium on Personal, Indoor and Mobile Radio Communications (PIMRC '06)*, pp. 1–5, Helsinki, Finland, September 2006.

[24] J. Choi, C. Lee, H. W. Jung, and Y. H. Lee, "Carrier frequency offset compensation for uplink of OFDM-FDMA systems," *IEEE Communications Letters*, vol. 4, no. 12, pp. 414–416, 2000.

[25] M. Schellmann and S. Stanczak, "Multi-user MIMO channel estimation in the presence of carrier frequency offsets," in *Proceedings of the 39th Asilomar Conference on Signals, Systems and Computers*, pp. 462–466, Pacific Grove, Calif, USA, October 2005.

[26] S. Ahmed, S. Lambotharan, A. Jakobsson, and J. Chambers, "MIMO frequency-selective channels with multiple frequency offsets: estimation and detection techniques," *IEE Proceedings: Communications*, vol. 152, no. 4, pp. 489–494, 2005.

[27] L. Häring, S. Bieder, and A. Czylwik, "Closed-form estimators of carrier frequency offsets and channels in the uplink of multiuser OFDM systems," in *Proceedings of IEEE International Conference on Acoustics, Speech and Signal Processing (ICASSP '06)*, vol. 4, pp. 661–664, Toulouse, France, May 2006.

[28] K.-H. Wu, W.-H. Fang, and J.-T. Chen, "Joint DOA-frequency offset estimation and data detection in uplink MIMO-OFDM networks with SDMA techniques," in *Proceedings of the 63rd IEEE Vehicular Technology Conference (VTC '06)*, vol. 6, pp. 2977–2981, Melbourne, Canada, May 2006.

[29] S. Sezginer and P. Bianchi, "Asymptotically efficient reduced complexity frequency offset and channel estimators for uplink MIMO-OFDMA systems," *IEEE Transactions on Signal Processing*, vol. 56, no. 3, pp. 964–979, 2008.

[30] V. Jungnickel, M. Schellmann, A. Forck, et al., "Demonstration of virtual MIMO in the uplink," in *IET Smart Antennas and Cooperative Communications Seminar*, London, UK, October 2007.

[31] M. Schellmann and V. Jungnickel, "Effects of multiple users' CFOs in OFDM-SDMA up-link: an interference model," in *Proceedings of IEEE International Conference on Communications (ICC '06)*, vol. 10, pp. 4642–4647, Istanbul, Turkey, June 2006.

[32] P. H. Moose, "Technique for orthogonal frequency division multiplexing frequency offset correction," *IEEE Transactions on Communications*, vol. 42, no. 10, pp. 2908–2914, 1994.

[33] T. M. Schmidl and D. C. Cox, "Robust frequency and timing synchronization for OFDM," *IEEE Transactions on Communications*, vol. 45, no. 12, pp. 1613–1621, 1997.

[34] J. H. Winters, J. Salz, and R. D. Gitlin, "The impact of antenna diversity on the capacity of wireless communication systems," *IEEE Transactions on Communications*, vol. 42, no. 234, part 3, pp. 1740–1751, 1994.

[35] S. M. Kay, *Fundamentals of Statistical Signal Processing, Volume 1: Estimation Theory*, Signal Processing Series, Prentice Hall PTR, Upper Saddle River, NJ, USA, 1993.